

# Synthesis and Characterization of Lithium-Doped Lanthanum Titanate Oxide Materials for the Fabrication of a Solid-State Microbattery Rectifier for Use in Direct Methanol Fuel Cell Powered Device

Steve De Cliff\*, Michael L. Post<sup>2</sup> and Isobel Davidson<sup>2</sup>

<sup>1</sup>University of Burundi, Faculty of Sciences, Department of Chemistry, 2 Unesco Avenue, P O Box 1550, Bujumbura, Burundi

<sup>2</sup>National Research Council of Canada, Institute for Chemical Process and Environmental Technology, Ottawa, Ontario K1A 0R6, Canada

**Abstract:** Materials required for the fabrication of a micro lithium-ion battery have been synthesized. Coin cells made of the above materials showed very promising features for future development of microbatteries. Solid electrolytes with high lithium conductivity may serve as useful components for enabling novel lithium ion battery system design. This work attempts to demonstrate the possible integration of lithium lanthanum titanate ( $\text{Li}_{0.390}\text{La}_{0.537}\text{TiO}_3$ ) materials into an all-solid battery system with  $\text{Li}[\text{Li}_{1/3}\text{Ti}_{5/3}]\text{O}_4$  as anode material in combination with a high voltage spinel of the family  $\text{Li}_2(\text{M}_1\text{M}_2)_x\text{Mn}_{3-x}\text{O}_8$  cathode, namely the  $\text{Li}_2\text{Co}_{0.4}\text{Fe}_{0.4}\text{Mn}_{3.2}\text{O}_8$  material. The cell operates along the expected voltage levels, demonstrating the feasibility of this concept in the advanced lithium-ion battery technology.

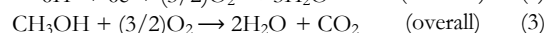
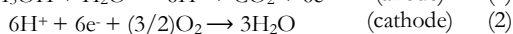
**Keywords:** Lithium-ion; Solid Electrolyte; Perovskite; Batteries; Microbatteries; Direct Methanol Fuel Cell; Fuel Cell

## 1. Introduction

### 1.1. Statement and Motivation for Fabricating a Lithium-Based Microbattery Rectifier

Recently, the demand for energy storage sources of high energy density has been growing rapidly as a result of the impetus of portable consumer electronics prevalence. Currently, more stringent requirements exist both in energy density and power density of energy storage devices in the large applications, such as zero emission electric vehicles and satellites. There is also a huge demand for high performance batteries. The fuel cells and secondary or rechargeable lithium-ion batteries are promising option to meet such demands because of their inherent outstanding characteristics.

A direct methanol fuel cell (DMFC) is a renewable energy source which works at near room temperature, and allows for easier liquid fuel storage, which makes it a potential candidate. Unlike a hydrogen polymer electrolyte fuel cell ( $\text{H}_2$ -PEMFC), the direct methanol fuel cell (DMFC) does not require ancillary components such as a separate humidifier, fuel processor, or cooling system. Within a DMFC, electricity is produced by a simple anodic/cathodic methanol oxidation/reduction reaction, shown as:



With the above reaction, even at 50% efficiency, one ml of methanol can deliver about 2.5 Watt-hours of electricity. Because of these qualities, DMFCs are ideally suited for electronic applications typically powered by electrochemical battery systems.

There have been significant ongoing activities in the United States, in Canada and elsewhere to develop large-scale DMFC technology. Preliminary studies have been performed on large-scale ( $> 1 \text{ cm}^2$  active area) DMFC systems at Jet Propulsion Laboratory (Surampudi *et al.*, 1994; Halpert *et al.*, 1997), at Los Alamos National Laboratory (Ren *et al.*, 2000; Ren and Gottesfeld, 2000) and at the Pennsylvania State University (Lu and Wang, 2005; Shaffer and Wang, 2010). While these studies on macro-systems show great promise of DMFC technology, its application to portable and Micro-Electromechanical System (MEMS) power sources is not straightforward, in view of the fundamental differences between macro- and micro-systems. At the beginning of this new millennium, several organizations including Motorola (Bostaph *et al.*, 2001), Jet Propulsion Laboratory (Narayanan *et al.*, 2001), the University of Minnesota (USA) (Kelly *et al.*, 2000) and the National Research Council of Canada (NRC) have undertaken aggressively research programs aimed to develop micro direct methanol fuel cells for MEMS applications.

Calculations on a micro direct methanol fuel cell system consisting of twenty cells with a total volume of  $1 \text{ cm}^3$  can deliver a power of 0.5-1.0 Watt (Mench *et al.*, 2001) and clearly show that adequate anode and cathode stoichiometries can be achieved. With an appropriate design, such micro-DMFCs are expected to provide a several-fold increase in specific energy than the best lithium-based thin film batteries.

However, while high methanol concentrations allow the attainment of higher power densities, this also results in increased fuel loss by crossover (Liu and Wang, 2009; Shaffer and Wang, 2009) and low fuel cell efficiency. Moreover, the power density and the rate of fuel crossover at a chosen cell voltage are strong functions of

\*Corresponding author. E-mail: steve.decliff@ub.edu.bi

the operating temperature. In short, the practical operation of micro-direct methanol fuel cell systems will depend on the performance of MEMS devices in terms of power consuming. As a result of the relatively poor performance projected so far, an advanced design of a small-scale lithium-based rectifier battery for use as a parallel power for this uncompensated power, at least to operate some electronic circuits has been suggested. But spontaneously, one can think that in an environment where several components that operate continuously at relatively high temperatures coexist, the presence of another liquid other than the fuel is unacceptable. This is because in the event of a leak, its vapors could interfere with those of the fuel, which could damage the entire system. Therefore, one key bottleneck for design and fabrication of an all-solid battery is the imperative need of replacement of the conventional liquid electrolyte by a solid one. This has stimulated interest in characterizing a variety of materials that can be used as solid electrolytes and electrode materials capable to accommodate sufficient ions for a better capacity and acceptable voltage.

The results presented in this paper are the findings of a preliminary study of a vast research program undertaken at the National Research Council of Canada (NRC) and aimed at the preparation of materials for the fabrication of a solid-state microbattery rectifier to be integrated in a MEMS powered by a direct methanol fuel cell (DMFC). In the present work, ABO<sub>3</sub>perovskite-type oxides, namely the lithium-doped lanthanum titanate oxides (LLTO) and some Li-based spinels were investigated and synthesized as possible materials for solid-state lithium-ion batteries.

One of the strategic economic applications behind the above research program is the fabrication of a MEMS device that can be used as a radio-frequency (RF) remote control system for pipelines installations monitoring or for various advanced defense applications.

In this paper, we report unpublished hitherto results first presented as a poster during an *Electrochemical Society Symposium* session held at the Queen University in Kingston, Ontario, Canada.

## 1.2. The Lithium-ion Batteries

The assessment criteria of batteries should be based on their most important features: open-circuit voltage, specific capacity, energy density, power density, charge and discharge characteristics, current-voltage diagram, energy efficiency, cycle life, and overcharge reactions. Among the above mentioned, the two major properties are energy density (Ampere.hour g<sup>-1</sup>) and power performance. The search for high energy density cells inevitably leads us to lithium, which is the lightest of all metallic elements (M.Wt. = 6.941 g mol<sup>-1</sup>, density = 0.534 g cm<sup>-3</sup>), and the most electropositive of the alkali metals (Mench *et al.*, 2001) and has also the highest absolute electrochemical potential E° = -3.045 V vs NHE (normal hydrogen electrode). These properties are responsible for the high gravimetric energy density of Li-

ion batteries. The theoretical energy density of Li metal is 3.86 Ah g<sup>-1</sup>, which is the highest (Hossain, 1995).

Lithium was initially employed in primary batteries; the concept of using Li-ions in a rechargeable cell came afterwards with the unexpected discovery of the Li insertion property of carbon in mid-1980's. This brought the breakthrough needed for the new battery system based on Li-ion concept, the so-called lithium-ion battery (LIB). The first primary LIBs became commercially available in 1991, by Sony Energetic Inc (Nishi, 1998). Since then, LIBs caught on quickly and have become the main power sources on the consumer electronics market (Broussely *et al.*, 1999). As an example, the sale volume of portable Li-ion batteries exceeded the total sale volume of all other types of batteries, such as NiCd and NiMH, in 1999 (Broussely *et al.*, 1999). Lithium-ion batteries are characterized by high specific energy and high specific power, which are the advantages that most other electrochemical energy storage technologies cannot offer. In addition, some other advantages such as high efficiency, long life cycle and low self-discharge rate make LIBs well suited for applications such as energy storage grid and electric transportation. Despite their overall advantages, scaling up LIB technology for these applications is still problematic due to safety, costs, operational temperature and availability of materials (Goodenough and Kim, 2011).

The desire to obtain high power performances of secondary batteries has spurred the development of variety of materials for electrodes and electrolytes. These materials include metals, metal hydrides, carbon, graphite and metal or earths rare oxides such as perovskites, liquids, polymers and solids for electrolytes.

## 1.3. The Solid Electrolyte Materials

The lithium lanthanum titanates, Li<sub>3x</sub>La<sub>2/3-x</sub>TiO<sub>3</sub> (LLTO), are a series of compounds which are themselves part of a subset of perovskites known as A-site deficient perovskites. Originally discovered by Brous (Brous *et al.*, 1953), members of this perovskite series were originally studied for their potential dielectric properties arising from displacements of the Ti<sup>4+</sup> cation. However, there was not a lot of success in this area due to another physical property which lead to the discovery of LLT's most impressive and significant application as a solid state electrolyte. Recent reports (Itoh *et al.*, 1994; Shan *et al.*, 1995; Kawakami *et al.*, 1998) show that some perovskite-type oxides containing rare earth metals exhibit very high lithium ionic conductivity at room temperature when they were used as cathodes for rechargeable lithium-ion batteries.

Among the best highest bulk lithium ion-conducting solid electrolyte known to date, the perovskite (ABO<sub>3</sub>)-type lithium lanthanum titanate, like (Li,La) TiO<sub>3</sub> (LLTO), with formulation Li<sub>3x</sub>La<sub>2/3-x</sub>TiO<sub>3</sub> and its layered derivatives, show the highest bulk lithium ion conductivities as high as 10<sup>-5</sup>-10<sup>-3</sup> S cm<sup>-1</sup> at room temperature (Bohnké *et al.*, 1996; Inaguma *et al.*, 1997;

Stramare *et al.*, 2003; Zou and Inoue, 2005; Bohnké, 2008; Mei *et al.*, 2008; Swamy *et al.*, 2013), which is 10 to 1000 times higher than amorphous lithium phosphorus oxy-nitride (LiPON) compositions. However, due to the high grain boundary resistance, the total has been conductivity lowered to about  $10^{-6}$ - $10^{-4}$  S cm<sup>-1</sup> (Latie *et al.*, 1984; Kawai and Kuwano, 1994; Inaguma *et al.*, 1994; Inaguma *et al.*, 1995; D'Andrea *et al.*, 2000; Panero *et al.*, 2000; Bonino *et al.*, 2001; Panero *et al.*, 2001; Takamura, 2002; Jimenez *et al.*, 2009; Inaguma *et al.*, 2010; Swamy *et al.*, 2013), which still be 1 to 100 times higher than LiPON compositions.

The actual mechanism of lithium ion conduction in the LLTO material is not yet clearly understood. The high lithium ion conductivity of LLTO is considered to be due to the large concentration of A-site vacancies and the motion of lithium by a vacancy mechanism through the wide square planar bottleneck between the A-sites. It is considered that BO<sub>6</sub>/TiO<sub>6</sub> octahedra tilting facilitate the lithium ion mobility in the perovskite structure. The activation energy for ionic conductivity in perovskite-type lithium ion-conducting oxides is essentially governed by structural distortions (Panero *et al.*, 2000) in which the larger Bion gives rise to structural distortion such as the tilt of the BO<sub>6</sub> octahedra, which decreases the bottleneck size, and the resultant smaller bottleneck determines the activation energies for ionic diffusion.

The ionic conductivity of LLTO is dependent on the size of the A-site ion cation (e.g., La or rare earth, alkali or alkaline earth), lithium and vacancy concentration and the nature of the B–O bond. For example, replacement of La by other rare earth elements with smaller ionic radii than that of La decreases the lithium ion conductivity, while partial substitution of La by Sr (larger ionic radii than that of La) slightly increases the lithium ion conductivity.

For lithium-doped lanthanum titanate materials, the lithium-ion conduction originates from vacancies located in the perovskite cages of  $\text{Li}_{3x}\text{La}_{2/3-x}\square_{1/3-2x}\text{TiO}_{3x}$ , ( $0 < x < 0.16$ ) through which Li<sup>+</sup> can migrate. Figure 1 shows a crystal structure of such perovskite with vacancies labeled by a square. For this material, the maximum ion conductivity was observed for  $x = 0.12 \pm 0.02$ . Two kinds of Li<sup>+</sup> movements were identified, one within the cages, and the other from cage to cage. These materials exist in two crystalline forms: the tetragonal form exhibits conductivity of  $1 \times 10^{-3}$  S cm<sup>-1</sup> at room temperature with an activation energy of 0.40 eV; the cubic form exhibits conductivity of  $2 \times 10^{-3}$  S cm<sup>-1</sup>. Both forms have a perovskite structure and their conductivity is comparable to that of commonly used polymer/liquid electrolytes.

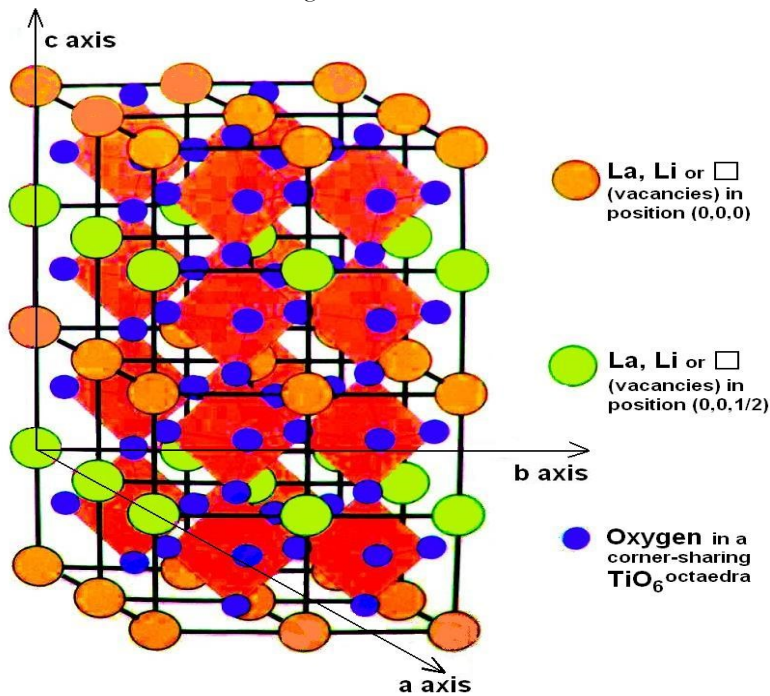


Figure 1. Crystal structure of the  $\text{Li}_{3x}\text{La}_{2/3-x}\square_{1/3-2x}\text{TiO}_{3x}$  perovskite material (drawn by ourselves).

It is worth to mention that the ionic conductivity of the Ti-based LLTO materials is highly sensitive to the lithium content. Noteworthy is that the compound is not stable in direct contact with elemental lithium and rapidly undergoes Li-insertion with consequent reduction of Ti<sup>4+</sup> to Ti<sup>3+</sup>, leading to high electronic

conductivity. Due to this reason, these materials cannot use lithium as anode material, unless Ti is substituted by Ta, then forming a completely new LLTO, namely  $\text{La}_{1/3-x}\text{Li}_{3x}\text{TaO}_3$ .

It has been observed that in the LLTO  $\text{Li}_{3x}\text{La}_{2/3-x}\square_{1/3-2x}\text{TiO}_{3x}$ , lithium intercalation starts to happen at 1.6 V vs

Li/Li<sup>+</sup> (electronic conductivity). These materials likely exhibit a high stability window over 5.5 V vs Li/Li<sup>+</sup>. Therefore, one of the requirements for use of these materials as solid electrolytes is the necessity of a high voltage anode material which can be able to intercalate lithium at voltage close to 1.6 V vs Li/Li<sup>+</sup>.

## 2. Materials and Methods

### 2.1. Requirements for the Anode and Cathode Materials

One of the known anode material which fulfills the abovementioned requirement is the spinel lanthanum titanate oxide (LTO) material, namely the Li<sub>4/3</sub>Ti<sub>5/3</sub>O<sub>4</sub> the lithium intercalation of which obeys the following reaction (Panero *et al.*, 2000; Bonino *et al.*, 2001; Scrosati *et al.*, 2002):



To be efficient, the above LTO material must be used with a high voltage cathode material. One material that fulfills such characteristics is the so-called high voltage mixed metals type oxides, namely the spinel Li<sub>2</sub>Fe<sub>x/2</sub>Co<sub>x/2</sub>Mn<sub>4-x</sub>O<sub>8</sub>. Bonino *et al.* (2001) and Panero *et al.* (2001) have optimized this material and observed two plateaus for x = 0.8, at 5.0V and 4.0V vs Li/Li<sup>+</sup>. Similarly, when combined in an electrochemical cell with the spinel Li<sub>4/3</sub>Ti<sub>5/3</sub>O<sub>4</sub>, two nominal voltages of 3.5V and 2.5V vs Li/Li<sup>+</sup>, are expected (Panero *et al.*, 2000; Panero *et al.*, 2001; Scrosati *et al.*, 2002).

With this in mind, we have undertaken a preliminary synthesis and characterization of some known perovskite-based materials for the fabrication of all-solid-state micro-batteries for use in electronics or in devices of micro electro-mechanical systems devices. The project was initiated in the NRC's laboratories and aimed to fabricate a microbattery rectifier for use in a micro-direct methanol fuel cell (μ-DMFC) powered device

### 2.2. Methods of Synthesis and Characterization

All battery materials were synthesized using the Ceramic Solid State synthesis route usually denoted as CSS in the literature (West, 1984a, 1984b; Cheetham and Day 1987; Keer, 1993; Wold and Dwight 1993). All X-ray diffraction measurements were performed on a Bruker D8 diffractometer using Cu-KD radiation. The diffractometer was equipped for parallel beam geometry with primary and secondary double Göbel mirrors. Most of the data was collected using a scan step size of 2θ = 0.02° with dwell time of 2 seconds per step. The film morphology was characterized by scanning electron microscopy (SEM) using a Philips XL 30S FEG-SEM at an acceleration voltage of 5kV.

### 2.3. Synthesis of Anode and Cathode Materials

The spinel-type Li[Li<sub>1/3</sub>Ti<sub>5/3</sub>]O<sub>4</sub> anode material and the spinel solid solution Li<sub>2</sub>Co<sub>0.4</sub>Fe<sub>0.4</sub>Mn<sub>3.2</sub>O<sub>8</sub> cathode

material were both synthesized using a wet dissolution procedure optimized by Scrosati *et al.* (2002), but in air instead of pure oxygen flux. The stoichiometry of the final anode and cathode compounds were determined by plasma atomic emission (IPC) as explained by the same authors.

Li[Li<sub>1/3</sub>Ti<sub>5/3</sub>]O<sub>4</sub> was prepared by dispersing stoichiometric amount of TiO<sub>2</sub> (Aldrich 99,9%) and LiOH.H<sub>2</sub>O (Aldrich) in n-hexane. After removing the solvent, the resulting powder was ground and calcined at 800 °C for 24 hours.

The synthesis of Li<sub>2</sub>Co<sub>0.4</sub>Fe<sub>0.4</sub>Mn<sub>3.2</sub>O<sub>8</sub> involved the mixing of water-acetic acid solutions of the precursors, i.e. LiOH.H<sub>2</sub>O (Aldrich), Mn(CH<sub>3</sub>COO)<sub>2</sub>.4H<sub>2</sub>O (Aldrich), Co(NO<sub>3</sub>)<sub>2</sub>.6H<sub>2</sub>O (Aldrich) and Fe(NO<sub>3</sub>)<sub>3</sub>.9H<sub>2</sub>O (Aldrich), followed by the evaporation to dryness and the annealing of the resulting powders. The solutions were stirred and evaporated to dryness at 120 °C. The resulting powders were ground and pre-calcined in air at 200 °C for 2 hours and at 300 °C for 10 hours. The solids were crushed and annealed under oxygen flux at 800 °C for 24 hours with slow-cooling and intermittent regrinding.

Cathode and anode materials used were black and white, respectively. Sinterability of Li<sub>2</sub>Fe<sub>0.4</sub>Co<sub>0.4</sub>Mn<sub>3.2</sub>O<sub>8</sub> was improved by further ball-milling to reduce the particle size (Figure 2).

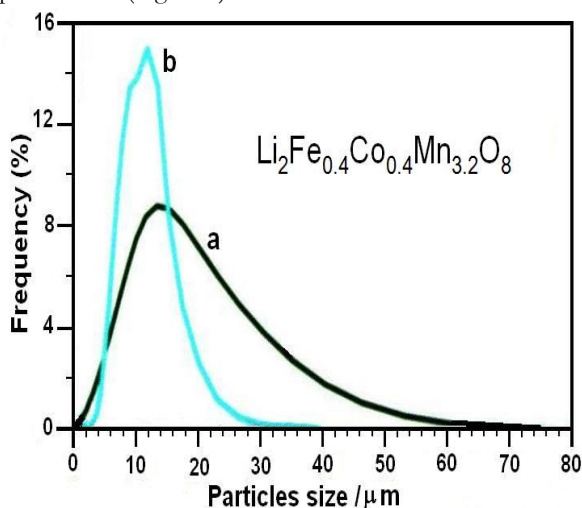


Figure 2. Particles size of the Li<sub>2</sub>Fe<sub>0.4</sub>Co<sub>0.4</sub>Mn<sub>3.2</sub>O<sub>8</sub> powder: a) As synthesized; and b) After 24 hours of ball-milling.

Figure 3 shows the SEM pictures of the spinel Li<sub>4/3</sub>Ti<sub>5/3</sub>O<sub>4</sub> and of the spinel Li<sub>2</sub>Fe<sub>0.4</sub>Co<sub>0.4</sub>Mn<sub>3.2</sub>O<sub>8</sub> and their x-ray diffraction patterns (Figure 4) show that all materials were single phase: the patterns reveal the high degree of crystallinity of the samples synthesized and confirm the purity and the high crystallinity of the two-electrode compounds.

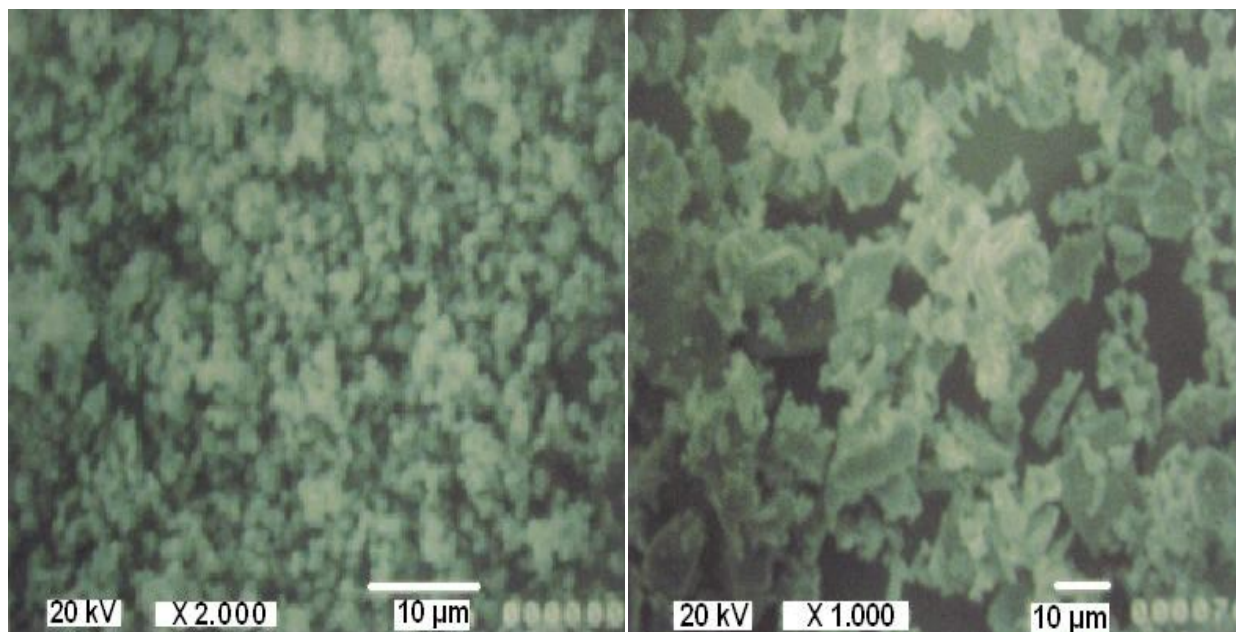


Figure 3. Scanning electron microscopy (SEM) pictures of the spinels  $\text{Li}[\text{Li}_{1/3}\text{Ti}_{5/3}]\text{O}_4$  (left) and  $\text{Li}_2\text{Fe}_{0.4}\text{Co}_{0.4}\text{Mn}_{3.2}\text{O}_8$  (right).

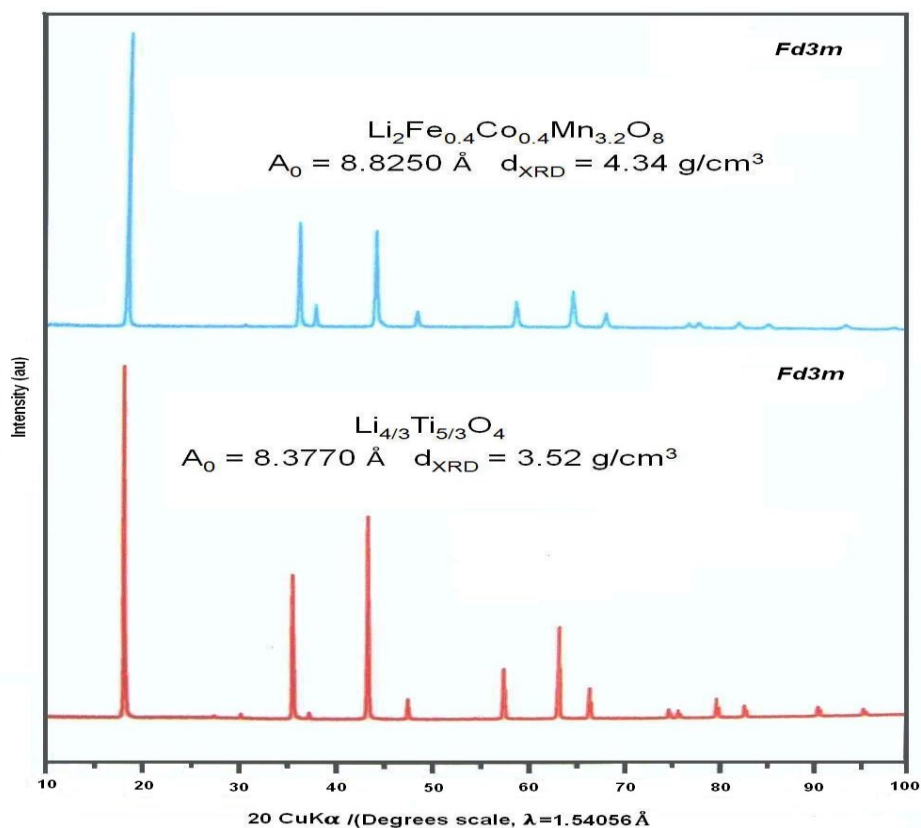


Figure 4. X-ray diffraction (XRD) patterns of  $\text{Li}_2\text{Fe}_{0.4}\text{Co}_{0.4}\text{Mn}_{3.2}\text{O}_8$  and  $\text{Li}[\text{Li}_{1/3}\text{Ti}_{5/3}]\text{O}_4$ .

#### 2.4. Synthesis of the Electrolyte Material

Keeping in mind the fact that a maximum conductivity for the LLTO materials exhibit a maximum conductivity for  $x = 0.12 \pm 0.2$ , a solid electrolyte component material

of the formula  $\text{Li}_{0.390}\text{La}_{0.537}\text{TiO}_3$  was first synthesized as a solid electrolyte material. This corresponds to  $x = 0.13$ . Precursor's materials for the synthesis of such a material were put in a mixture of  $\text{La}_2\text{O}_3$ ,  $\text{Li}_2\text{CO}_3$  and  $\text{TiO}_2$ . Such

mixture was heated in an oven at 900 °C for 4 hours. Ball-milling was performed in EtOH for 18 hours in order to reduce the particle size of the fired material and then re-fired at 800 °C for 4 hours. During sintering, the fired material was successively kept at 1050 °C for 12

hours, and again at 1230 °C for another 12 hours. During firing, the heating and cooling rate was 0.2 °C per minute. Both quenching and cooling were performed (Figure 5).

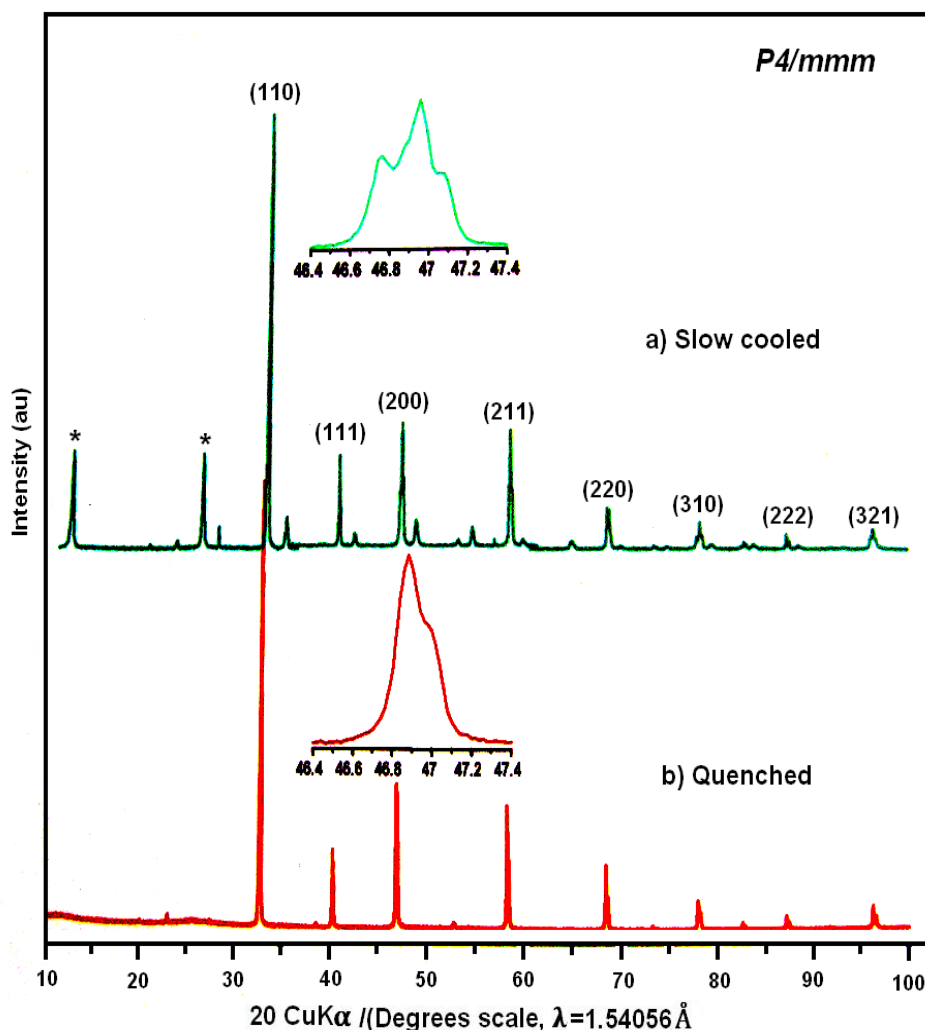


Figure 5. X-ray diffraction (XRD) patterns of  $\text{Li}_{0.390}\text{La}_{0.537}\text{TiO}_3$  forms: a) Tetragonal (ordered) form prepared by simple slow cooling; and b) Cubic (disordered) form prepared by quenching.

The synthesized LLTO material is beige but the color seems to degrade in contact with air after sometimes. X-ray patterns of the powder of the synthesized LLTO electrolyte material are shown in Figure 5. Ordered forms of LLTO (mixture of cubic, tetragonal and orthorhombic) were obtained by slow cooling. The crystal structure is orthorhombic with space group  $P4mmm$ . Disordered form (~95% cubic) were also obtained by simple quenching in air. Pellets of LLTO showed a very good sinterability (30% shrinking).

### 3. Results and Discussion

In our investigation, we have considered the  $\text{LiPF}_6\text{-PC}$  electrolyte, an electrolyte solution formed by dissolving  $\text{LiPF}_6$  in propylene carbon, PC, i.e., by selecting the salt

and the solvent which are expected to be the most stable candidates among the known lithium liquid electrolyte materials.

Synthesized and characterized materials were assembled in separate coin cells with slurry mixtures of active materials made by tape casting using a “doctor blade”. These coin cells were assembled and sealed in a glove box chamber. Three series (A, B and C) of coin cells batteries were assembled and cycled:

- A.  $\left| \text{Li}_{4/3}\text{Ti}_{5/3}\text{O}_4 \right| \text{LiPF}_6\text{-PC} \left| \text{Li} \right|$
- B.  $\left| \text{Li}_2\text{Co}_{0.4}\text{Fe}_{0.4}\text{Mn}_{3.2}\text{O}_8 \right| \text{LiPF}_6\text{-PC} \left| \text{Li} \right|$  and
- C.  $\left| \text{Li}_{4/3}\text{Ti}_{5/3}\text{O}_4 \right| \text{LiPF}_6\text{-PC} \left| \text{Li}_2\text{Co}_{0.4}\text{Fe}_{0.4}\text{Mn}_{3.2}\text{O}_8 \right|$

The absence of a major structural deformation is once again confirmed as it has been observed by other authors (D'Andrea *et al.*, 2000; Mei *et al.*, 2008; Jimenze *et al.*, 2009; Inaguma *et al.*, 2010). This makes  $\text{Li}[\text{Li}_{1/3}\text{Ti}_{5/3}]\text{O}_4$  an almost “zero strain” electrode material characterized by a very good cyclability and by a very little capacity fade upon cycling. This is confirmed by the cycling responses reported in Figure 6 for which cycling responses of  $\text{Li}[\text{Li}_{1/3}\text{Ti}_{5/3}]\text{O}_4$  showed high reversibility and fast kinetics of the intercalation/de-intercalation process:

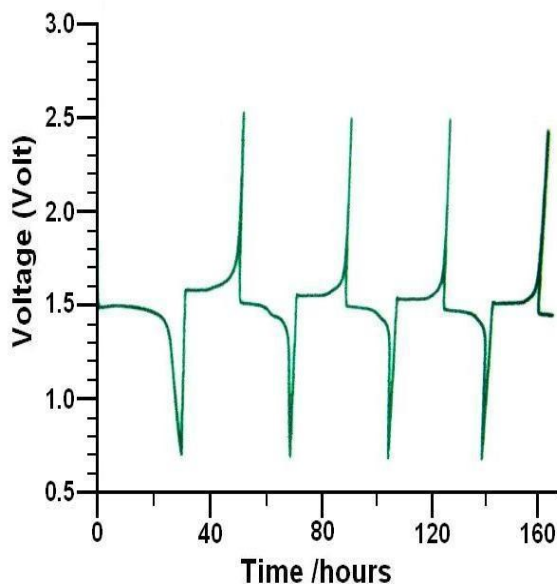
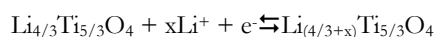


Figure 6. Typical voltage profile of a charge-discharge cycle of  $\text{Li}[\text{Li}_{1/3}\text{Ti}_{5/3}]\text{O}_4$  electrode in a coin cell working in the  $\text{LiPF}_6\text{-PC}$  electrolyte and Li as counter electrode; at room temperature.

This process involves one lithium equivalent per formula and clearly evolves around 1.5 V vs Li with high reversibility, fast kinetics and with very stable capacity delivery for all C-rates applied. In the case of the  $\text{Li}_2\text{Fe}_{0.4}\text{Co}_{0.4}\text{Mn}_{3.2}\text{O}_8$  cells using the  $\text{LiPF}_6\text{-PC}$  solution electrolyte, two plateaus are identified (Figure 7). The voltage-capacity trends demonstrate the two stages of the Li intercalation/de-intercalation:

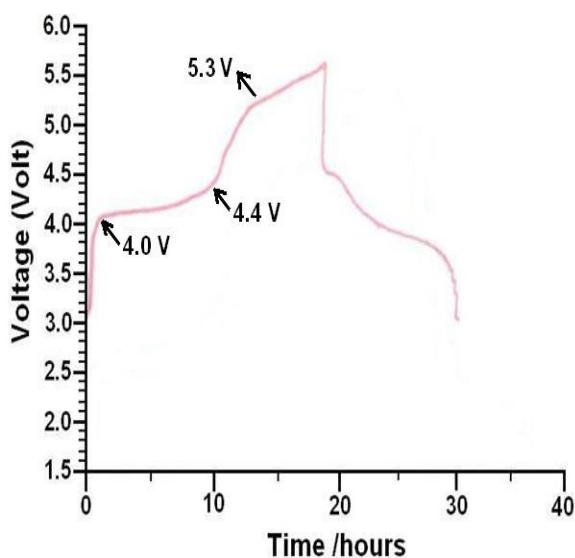


Figure 7. Typical voltage profile of a charge-discharge cycle of  $\text{Li}_2\text{Co}_{0.4}\text{Fe}_{0.4}\text{Mn}_{3.2}\text{O}_8$  electrode in a coin cell working in the  $\text{LiPF}_6\text{-PC}$  electrolyte and Li as counter electrode; at room temperature.

Electrochemical process, which evolves along a first plateau is said to be associated with the Mn redox process around 4 V, followed by a second plateau evolving around 5 V vs Li. The extent of the high voltage second plateau depends on the type of the M metals. The two plateaus are reversible, suggesting fast kinetics for both processes. The same two plateaus are again observed with a cell made of a combination of these two above spinels materials, namely the  $\text{Li}_2\text{Fe}_{0.4}\text{Co}_{0.4}\text{Mn}_{3.2}\text{O}_8$  and the  $\text{Li}_{4/3}\text{Ti}_{5/3}\text{O}_4$  using the  $\text{LiPF}_6\text{-PC}$  solution electrolyte (Figure 8).

Finally, even if the LLTO/LTO cell system showed good charge/discharge characteristics over 100 cycles at 60 °C, as expected, the nominal voltages are lowered by 1.5 V and the  $\text{LiPF}_6\text{-PC}$  electrolyte seems to suffer decomposition when held at voltages higher than 4.4 V. This is observed for both the  $\text{Li}_2\text{Fe}_{0.4}\text{Co}_{0.4}\text{Mn}_{3.2}\text{O}_8/\text{Li}$  and the  $\text{Li}_2\text{Fe}_{0.4}\text{Co}_{0.4}\text{Mn}_{3.2}\text{O}_8/\text{Li}_{4/3}\text{Ti}_{5/3}\text{O}_4$  systems (Figures 7 and 8). Thus, a definite decay in capacity is predicted when the cells are cycled at lower rates, i.e. at regimes which involve longer holding times at the high voltage range. Clearly, the use of these cathode materials requires the availability of an electrolyte solution having a stability window large enough to allow it to operate at and over 5 V. Unfortunately, unless the LLTO perovskite material reveals itself as likely being one of these electrolytes, the choice of liquid electrolytes having high oxidation stability is presently restricted to few cases and even these are not always completely satisfactory.

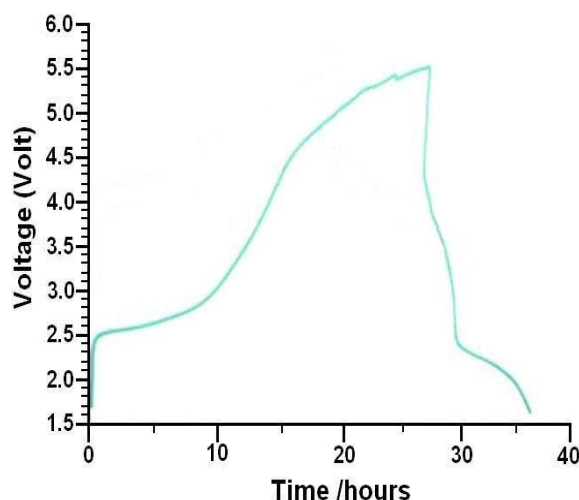


Figure 8. Typical voltage profile of a charge-discharge cycle of  $\text{Li}_2\text{Co}_{0.4}\text{Fe}_{0.4}\text{Mn}_{3.2}\text{O}_8$  electrode in a coin cell working in the  $\text{LiPF}_6\text{-PC}$  electrolyte and  $\text{Li}[\text{Li}_{1/3}\text{Ti}_{5/3}\text{O}_4]$  as counter electrode; at room temperature.

#### 4. Conclusions

Materials required for the fabrication of a micro lithium-ion battery have been synthesized. Coin cells made of the above materials showed very promising features for future development of microbatteries. The results reported here show that lithium can be extracted from the  $\text{Li}_2\text{M}_{0.4}\text{Mn}_{0.4}\text{O}_8$  spinel structure along two main potential regions which vary around 4.0-4.4 V and 4.4-5.3 V vs Li. Presently, the full exploitation of these 5 V cathodes materials is somewhat hindered by the lack of suitable electrolyte media. Future works in an all-solid-state battery based on the Li-ion technology should focus on the extensive characterization of the LLTO material in order to determine whether or not this solid electrolyte is really and undoubtedly stable in the voltage range of 2.5 V and 5.5 V or over. It is only afterwards that one can envisage the preparation of target materials for films deposition by either pulsed laser deposition (PLD) or by electrostatic spray deposition (ESD), with the objective of the fabrication of effective micro lithium-ion batteries and their integration in a variety of micro-electromechanical systems (MEMS) devices. What should be the sequential deposition of microbattery components on a chemically etched Si substrate has been designed and presented elsewhere.

#### 5. Acknowledgement

This research work was performed at the National Research Council of Canada (NRC) in the laboratories of the Energy Materials Group of the Institute for Chemical Process and Environmental Technology (NRC-ICPET) and in the Institute for Fuel Cell Innovation (NRC-IFCI). This work was financially supported by the Natural Sciences and Engineering Research Council of Canada (NSERC) through a

collaborative research program between NSERC and NRC.

#### 6. References

- Bohnké, O. 2008. The fast lithium-ion conducting oxides  $\text{Li}_{3x}\text{La}_{2/3-x}\text{TiO}_3$  from fundamentals to application. *Solid State Ionics* 179 (1-6): 9-15.
- Bohnké, O., Bohnké, C. and Fourquet, J.L. 1996. Mechanism of ionic conduction and electrochemical intercalation of lithium into the perovskite lanthanum lithium titanate. *Solid State Ionics* 91(1-2): 21-31.
- Bonino, F., Panero, S., Satolli, D. and Scrosati, B. 2001. Synthesis and characterization of  $\text{Li}_2\text{M}_x\text{Mn}_{4-x}\text{O}_8$  ( $\text{M}=\text{Co}, \text{Fe}$ ) as positive active materials for lithium-ion cells. *Journal of Power Sources* 97-98: 389-392.
- Bostaph, J., Koriipella, R., Fisher, A., Zindel, D., Hallmark, J. and Neutzler, J. 2001. Microfluidic fuel delivery for 100mW DMFC. *In: Proceedings of the Symposium on Direct Methanol Fuel Cells: The 199th Electrochemical Society Proceedings Series*, Princeton, NJ, USA, 2001.
- Brous, J., Fankuchen, I. and Banks, E. 1953. Rare earth titanates with a perovskite structure. *Acta Crystallographia* 6: 67-70.
- Broussely, M., Biensan, P. and Simon, B. 1999. Lithium insertion into host materials: the key to success for Li ion batteries. *Electrochimica Acta* 45 (1-2): 3-22.
- Cheetham, A.K. and Day, P. 1987 (Eds.). *Solid State Chemistry: Techniques*. Clarendon Press, Oxford University Press, UK.
- D'Andrea, S.D., Panero, S., Reale, P., and Scrosati, B. 2000. Advanced lithium ion battery materials. *International Journal of Ionics* 6:127-132.
- Goodenough, J.B. and Kim, Y. 2011. Challenges for rechargeable Li batteries. *Journal of Power Sources* 196(16): 6688-6694.
- Halpert, G., Narayanan, S.R., Valdez, T.I., Chun, W., Frank, H., Kinder, A. and Surampudi, S. 1997. Progress with the direct methanol liquid-feed fuel cell system. *In: Proceedings of the 32nd International Energy Conversion Engineering Conference (IECEC)* 2: 774-778.
- Inaguma, Y., Chen, L., Itoh, M. and Nakamura, T. 1994. Candidate compounds with perovskite structure for high lithium ionic conductivity. *Solid State Ionics* 70-71: 196-202.
- Inaguma, Y., Katsumata, T. and Mori, D. 2010. Predominant factor of activation energy for ionic conductivity in perovskite-type lithium ion-conducting oxides. *Journal of the Physical Society of Japan, Supplements* 79: 69-71.
- Inaguma, Y., Matsui, Y., Shan, Y.J., Itoh, M. and Nakamura, T. 1995. Lithium ion conductivity in the perovskite-type  $\text{LiTaO}_3\text{-SrTiO}_3$  solid solution. *Solid State Ionics* 79: 91-97.
- Inaguma, Y., Matsui, Y., Yu, J., Shan, Y., Nakamura, T. and Itoh, M. 1997. Effect of substitution and pressure on lithium ion conductivity in perovskites



- $\text{Ln}_{1/2}\text{Li}_{1/2}\text{TiO}_3$  (Ln = La, Pr, Nd and Sm). *The Journal of Physics and Chemistry of Solids* 58 (6): 843-852.
- Itoh, M., Inaguma, Y., Jung, W.H., Chen, L. and Nakamura T. 1994. High lithium ion conductivity in the perovskite-type compounds  $\text{Ln}_{1/2}\text{Li}_{1/2}\text{TiO}_3$  (Ln=La, Pr, Nd, Sm). *Solid State Ionics* 70-71: 203-207.
- Jimenez, R., Rivera, A., Varez, A. and Sanz, J. 2009. Li mobility in  $\text{Li}_{0.5-x}\text{Na}_x\text{La}_{0.5}\text{TiO}_3$  perovskites ( $0 < x < 0.5$ ). *Solid State Ionics* 180 (26-27): 1362-1371.
- Kawai, H. and Kuwano, J. 1994. Lithium ion conductivity of A-Site deficient perovskite solid solution  $\text{La}_{0.67-x}\text{Li}_{3x}\text{TiO}_3$ . *Journal of the Electrochemical Society* 141 (7): L78-L79.
- Kawakami, Y., Fukuda, M., Ikuta, H. and Wakihara, M. 1998. Ionic conduction of lithium for perovskite type compounds,  $(\text{Li}_{0.05}\text{La}_{0.317})_{1-x}\text{Sr}_{0.5x}\text{NbO}_3$ ,  $(\text{Li}_{0.1}\text{La}_{0.3})_{1-x}\text{Sr}_{0.5x}\text{NbO}_3$  and  $(\text{Li}_{0.25}\text{La}_{0.25})_{1-x}\text{M}_{0.5x}\text{NbO}_3$  (M = Ca and Sr). *Solid State Ionics* 110(3-4): 187-192.
- Keer, H.V. 1993. *Principles of the Solid State*, John Wiley & Sons, Inc., New Delhi, India.
- Kelly, S.C., Deluga, G.A. and Smyrl, W. 2000. A miniature methanol polymer electrolyte fuel cell. *Electrochemical and Solid State Letters* 3 (9): 407-409.
- Latie, L., Villeneuve, G., Conte, D. and Flem, G.L. 1984. Ionic conductivity of oxides with general formula  $\text{Li}_x\text{Ln}_{1/3}\text{Nb}_{1-x}\text{Ti}_x\text{O}_3$  (Ln = La, Nd). *Journal of Solid State Chemistry* 51(3): 293-299.
- Liu, F. and Wang, C.Y. 2008. Water and methanol crossover in direct methanol fuel cells - effect of anode diffusion Media. *Electrochimica Acta* 53: 5517-5522.
- Liu, F.Q. and Wang, C.Y. 2009. Dramatic reduction of water crossover in direct methanol fuel cells by cathode humidification. *Electrochemical and Solid-State Letters* 12: B101-B102.
- Lu, G.Q. and Wang, C.Y. 2005. Development of micro direct methanol fuel cells for high power applications. *Journal of Power Sources* 144: 141-145.
- Mei, A., Wang, X., Feng, Y., Zhao, S., Li, G., Geng, H., Lin, Y. and Nan, C. 2008. Enhanced ionic transport in lithium lanthanum titanium oxide solid state electrolyte by introducing silica. *Solid State Ionics* 179 (39): 2255-2259.
- Mench, M.M., Wang, Z.H., Bhatia, K. and Wang, C.Y. 2001. Design of a micro direct methanol fuel cell ( $\mu\text{DMFC}$ ). In: Proceedings of the IMECE'01 International Mechanical Engineering Congress and Exposition (IMECE). 11-16 November, 2001, New York, USA.
- Narayanan, S.R., Clara, F. and Valdez, T.I. 2001. Development of a miniature direct methanol fuel cell system for cellular phone applications. In: Proceedings of the Symposium on Direct Methanol Fuel Cells: the 199<sup>th</sup> Electrochemical Society Proceedings Series, Princeton, NJ, USA.
- Nishi, Y. 1998. *Advances in lithium-ion batteries*. In: Lithium Ion Batteries, Wakihara M. and Yamamoto O. (eds.). Kodansha Ltd., Tokyo, Japan. pp. 181.
- Panero, S., Reale, P., Ronci F., Scrosati B., Perfetti, P. and Rossi, A.V. 2001. Refined, *in situ* EDXD structural analysis of the  $\text{Li}[\text{Li}_{1/3}\text{Ti}_{5/3}]\text{O}_4$  electrode under lithium insertion-extraction. *Physical Chemistry Chemical Physics* 3(5): 845-847.
- Panero, S., Satolli, D., Salomon, M. and Scrosati, B. 2000. A new type of lithium-ion cell based on the  $\text{Li}_4\text{Ti}_5\text{O}_{12}/\text{Li}_2\text{Co}_{0.4}\text{Fe}_{0.4}\text{Mn}_{3.2}\text{O}_8$  high voltage electrode combination. *Electrochemistry Communications* 2(11): 810-813.
- Ren, X. and Gottesfeld, S. 2000. Electro-osmotic drag of water in poly (perfluorosulfonic acid) membranes. *Journal of the Electrochemical Society* 148: A87.
- Ren, X., Springer, T.E. and Gottesfeld, S. 2000. Water and methanol uptakes in Nafion membrane and membrane effects on direct methanol cell performance. *Journal of the Electrochemical Society* 147: 96.
- Scrosati, B., Panero, S., Reale, P., Satolli, D. and Aihara, Y. 2002. Investigation of new types of lithium-ion battery materials. *Journal of Power Sources* 105(2): 161-168.
- Shaffer, C.E. and Wang, C.Y. 2009. *Performance modeling and cell design for high concentration methanol fuel cells*: In: Handbook of Fuel Cells. V 6, Chpt. 50, pp. 749-461, John Wiley and Sons, Inc.
- Shaffer, C.E. and Wang, C.Y. 2010. High concentration methanol fuel cells: Design and Theory. *Journal of Power Sources* 195: 4185-4195.
- Shan, Y.J., Chen, L., Inaguma, Y., Itoh, M. and Nakamura, T. 1995. Oxide cathode with perovskite structure for rechargeable lithium batteries. *Journal of Power Sources* 54(2): 397-402.
- Stramare, S., Thangadurai, V. and Weppner, W. 2003. Lithium lanthanum titanates: A Review. *Chemistry of Materials* 15: 3974-3990.
- Surampudi, S., Narayanan, S.R., Vamos, E., Frank, H., Halpert, G., La Conti, A., Kosek, J., Surya Prakash G.K. and Olah, G.A. 1994. Advances in direct oxidation methanol fuel cells. *Journal of Power Sources* 47: 377-385.
- Swamy, D.T., Babu, K.E. and Veeraiiah, V. 2013. *Evidence for high ionic conductivity in lithium-lanthanum titanate,  $\text{Li}_{0.29}\text{La}_{0.57}\text{TiO}_3$* . *Bulletin of Materials Sciences* 36 (6): 1115-1119.
- Takamura, T. 2002. Trends in advanced batteries and key materials in the new century. *Solid State Ionics* 152-153: 19-34.
- West, A.R. 1984a. *Solid State Chemistry and its Applications*. John Wiley & Sons, Inc.
- West, A.R. 1984b. *Basic Solid State Chemistry*. John Wiley & Sons, Inc.
- Wold, A. and Dwight, K. 1993. *Solid State Chemistry. Synthesis, Structure, and Properties of Selected Oxides and Sulfides*. Chapman & Hall, New York, USA.
- Zou, Y. and Inoue, N. 2005. Structure and lithium ionic conduction mechanism in  $\text{La}_{4/3-y}\text{Li}_{3y}\text{Ti}_2\text{O}_6$ . *International Journal of Ionics* 11 (5-6): 333-342.

